Interaction and Multiscale Mechanics, Vol. 4, No. 4 (2011) 291-311
DOI: http://dx.doi.org/10.12989/imm.2011.4.4.291

Large-scale and small-scale self-excited torsional vibrations of homogeneous and sectional drill strings

V.I. Gulyayev* and O.V. Glushakova

Department of Mathematics, National Transport University, Suvorov str., 1 Kiev, 01010, Ukraine

(Received April 26, 2011, Revised July 4, 2011, Accepted July 9, 2011)

Abstract. To simulate the self excited torsional vibrations of rotating drill strings (DSs) in vertical bore-holes, the nonlinear wave models of homogeneous and sectional torsional pendulums are formulated. The stated problem is shown to be of singularly perturbed type because the coefficient appearing before the second derivative of the constitutive nonlinear differential equation is small. The diapasons $\omega_b \le \omega \le \omega_l$ of angular velocity ω of the DS rotation are found, where the torsional auto-oscillations (of limit cycles) of the DS bit are generated. The variation of the limit cycle states, i.e. birth ($\omega = \omega_b$), evolution ($\omega_b < \omega < \omega_l$) and loss ($\omega = \omega_l$), with the increase in angular velocity ω is analyzed. It is observed that firstly, at birth state of bifurcation of the limit cycle, the auto-oscillation generated proceeds in the regime of fast and slow motions (multiscale motion) with very small amplitude and it has a relaxation mode with nearly discontinuous angular velocities of elastic twisting. The vibration amplitude increases as ω increases, and then it decreases as ω approaches ω_l. Sectional drill strings are also considered, and the conditions of the solution at the point of the upper and lower section joints are deduced. Besides, the peculiarities of the auto-oscillations of the sectional DSs are discussed.

Keywords: drill strings; multiscale dynamics; relaxation vibration; singularly perturbed problem; torsional vibration.

1. Introduction

At the present time, the main sources of energy are oil and gas heat carriers whose cost grows steeply in connection with their approaching depletion. Nevertheless, reconnaissance of new oil and gas reserves and progressively increasing rate of their extraction continue. In so doing, the principal technological component of these processes is the drilling of new oil and gas holes. Nowadays even though their depths can reach several kilometers, the problem of oil and gas mining from deeper tectonic levels becomes more challenging.

When the fuel extraction is realized from great depths, the drill efficiency is associated with the problem of exposure to the emergency regimes of the DS functioning. Among these are the DS stability loss at its lower part, following the buckling mode typical for a rectilinear rod stretched, compressed and twisted simultaneously (Gulyayev *et al*. 2009) and the frictional seizure of the DS inside the curvilinear bore-hole (Gulyayev *et al*. 2011).

* Corresponding author, Professor, E-mail: valery@gulyayev.com.ua

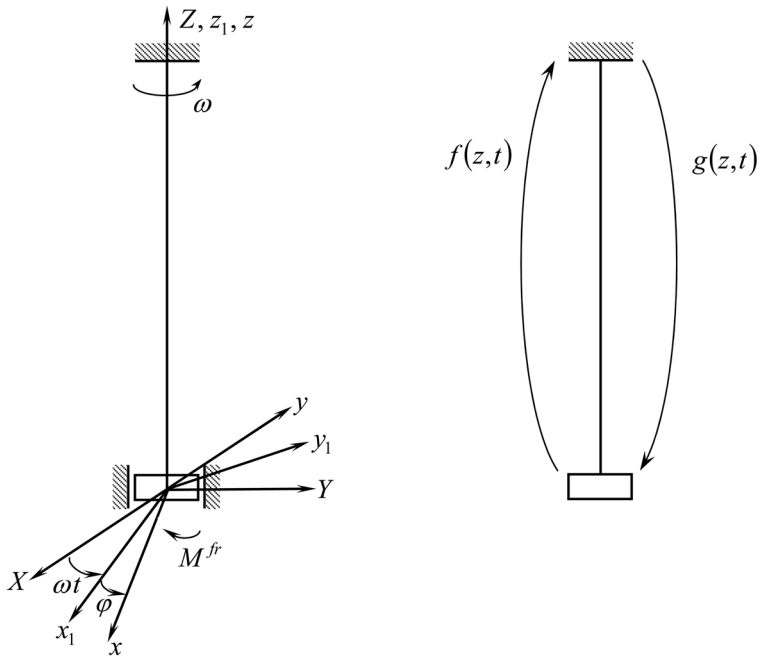

Fig. 1 Schematic of the drill string: (a) coordinate systems and (b) propagation of torsional waves

One of the dynamic phenomena resulting in the occurrence of emergency situation during drilling is the self-excitation of torsional vibrations of the rotating drill strings (Brett 1992, Challamel 2000, Leine *et al.* 2002, Mihajlovic *et al.* 2006, Tucker and Wang 1999, Zamanian *et al.* 2007). Inasmuch as a drill string represents a torsional pendulum (Fig. 1(a)) with energy outflow due to the dissipative interaction between the bit and broken rock at its lower part, it can transit from the stationary rotational state to the mode of torsional auto-oscillation. These vibrations are considered to be the most detrimental type to the service life of the drill string and downhole equipment, because they may induce large cyclic stresses, reduction of the bit life, unexpected changes in drilling direction, and even result in failure of the drill string.

The aforementioned phenomenon can be described by complicated non-linear differential equations, belonging to the so called singularly perturbed type (Gulyaev *et al.* 2010). Many mathematical models adequately describe the physical processes by the differential equation terms, involving (implicitly or explicitly) different parameters affecting the solution mode.

Beginning from the classic works by A. Poincare and A.M. Liapunov, the so called regular type of equations

$$x'' = F(t, x, x', \varepsilon) \qquad (0 \le t \le 1) \tag{1}$$

was profoundly studied. Here the right-hand part regularly (continuously, smoothly, analytically) depends on the parameter ε in the vicinity of $\varepsilon = 0$ and the solutions were studied inside the finite region $0 \le t \le 1$ of the independent variable t.

But the situation is widely diversified and complicated when the small parameter $0 < \varepsilon << 1$ appears before the second derivative

$$\varepsilon x'' = F(t, x, x') \qquad (0 \le t \le 1) \tag{2}$$

In this case, the influence of the left-hand part on the solution becomes significant only for large values of x'', related to the states of fast change in the system motion.

An effort to regularize Eq. (2) with small ε by discarding the term $\varepsilon x''$ leads to the regular differential equation

$$F(t, x, x') = 0 \qquad (0 \le t \le 1) \tag{3}$$

which, nevertheless, is of lower order and, for this reason, loses the basic features of the original Eq. (2).

Replacing the independent variable t with the substitutions $t = \sqrt{\varepsilon}\tau$ and $\frac{d^2x}{dt^2} = \frac{d^2x}{\varepsilon d\tau^2}$, which enables us to exclude parameter ε

$$\varepsilon \frac{d^2x}{dt^2} = \varepsilon \frac{d^2x}{\varepsilon d\tau^2} = \frac{d^2x}{d\tau^2} = F\left(\tau, x, \frac{dx}{d\tau}\right) \tag{4}$$

which is just the same, causing enlargement of the integration domain $0 \le \tau \le 1/\sqrt{\varepsilon}$ in comparison with the initial domain $0 \le t \le 1$.

The problems of the theory of differential equations with a small parameter appearing before the senior derivatives were given the title of singularly perturbed ones (Chang and Howes 1984, Shishkin and Shishkina 2009). As a rule, they have irregular solutions with nearly discontinuous derivatives. It is believed that L. Prandle was the first one to attract attention to this scientific direction in connection with the applied problem of boundary layers in hydrodynamics in 1904. Subsequently, the singularly perturbed problems emerged repeatedly in physics, mechanics and technology. Their distinguishing feature for the oscillatory systems is that they have periodic solutions in the shape of broken straight lines (Fig. 2) with rectangular phase portraits (Fig. 3). The vibrations of this type are called relaxation (Mishchenko and Rozov 1975). Among these are the periodic motions occurring under the action of nonlinear dissipative perturbations in autovibrational systems with small inertance.

In mechanical systems, these perturbations are the forces of internal and external friction, in electric systems the electric resistance. Every period of the relaxation vibrations can be divided into several separate segments corresponding to slow and fast changes of the system states, interpreted as multiscale ones. The nature of these vibrations is connected with small masses of the oscillatory systems (characterized by the small ε), which gives the condition for small inertance of the oscillators and the possibility of nearly instantaneous change of their velocities.

Simplified consideration of the relaxation vibration emergence is achieved by ignoring the system parameters affecting the character of fast motions, based on the so called degenerated type of equations as given in Eq. (3). Their use leads to distortion of the periodic motion mode.

Relaxation vibrations in electric systems are widely employed in measuring the devices, telecontrol, automatics and other divisions of electronics. Different generators, such as the blocking generators, multivibrators, RC-generators and others, are used for their excitations.

Their investigation was begun in the 20-th years of the last century in the works by Van-Der-Pole. Relaxation vibrations of this direction are profoundly studied owing to the possibility of application

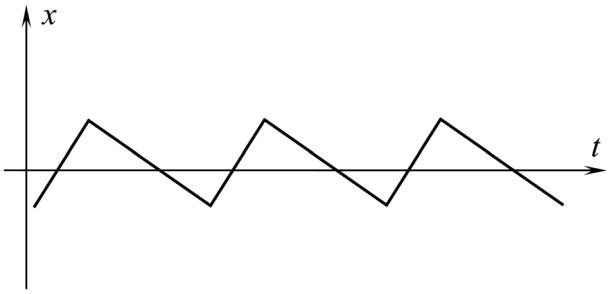

Fig. 2 Typical mode of relaxation vibration

of the analogue simulation method to their analysis.

In mechanics, the small inertance vibrational systems are rarely met. There are no universal methods for their investigation, because of this, they are poorly understood. An example of the singularly perturbed problems in mechanics, which plays a large role in practical applications, is the problem about the torsional auto-oscillations of long drill strings at their rotation with angular velocity ω. Such vibrations are generated as a consequence of nonlinear frictional interaction of their bits with the bore-hole bottom surfaces at the rock cutting. By virtue of the fact that the bit mass is much less than the drill string mass, the coefficient before the inertia member (the second derivative) of the appropriate vibration equation is very small and its solution has the shape of a broken line. In connection with the discontinuous character of the relaxation vibrations, they are dangerous for the strength of the bit and drill string.

In the paper by Gulyaev *et al.* (2010), the theoretical simulation of the homogeneous drill string auto-oscillation excitation was presented on the basis of the wave model of a torsion pendulum. It is observed that zones of change in parameter ω, where the auto-oscillations are excited, are bordered by the states of the limit cycle birth ω_b and loss ω_l. The vibrations are shown to be of the relaxation type and, what is more, have the character quantized in time with large- and small-scale regimes of motions. Similar phenomena are discussed by Kaczmarek (2010) and Wang and Fang (2010). The present paper is devoted to the analysis of the features of the auto-oscillation mode evolution in the vicinities of the bifurcational states and inside of the diapason $\omega_b < \omega < \omega_l$. Homogeneous and sectional drill strings are under consideration.

2. Constitutive equation of torsional vibrations of a homogeneous drill string

For the purpose of theoretically simulating the phenomenon of self-excitation of the torsional vibration of a drill string, the wave model of a torsional pendulum is used (Gulyaev *et al.* 2010). It is assumed that in the considered case the DS top end is driven with constant angular velocity ω relative to the inertial coordinate system OXYZ whose axis OZ is in line with the DS axis (Fig. 1(a)).

The DS is considered as an elastic rod in torsion. The twist vibrations of the system are excited through the frictional interaction of the DS bit with the broken rock at the bore-hole bottom. Assume that the moment of these forces far exceeds the distributed friction moments induced by viscous friction interaction of the DS body with ambient mud. So the last-mentioned ones can be neglected in analysis.

To describe the bit twist, let us introduce also the coordinate system Oxyz rotating with speed ω. Then the angle of the bit rotation relative to system OXYZ is $\omega t + \varphi(0, t)$, where ωt is the angle of the DS top end rotation; t is the time; $\varphi = \varphi(z, t)$ is the angle of the elastic twist of the DS element with respect to the Oxyz system.

By treating the elongated body of the DS rod as an elastic waveguide, its torsional vibrations can be modeled by the wave equation

$$\rho I_z \frac{\partial^2 \varphi}{\partial t^2} - G I_z \frac{\partial^2 \varphi}{\partial z^2} = 0 \tag{5}$$

where I_z is the inertia moment of the DS cross-section area, ρ is the material density, and G is the shear modulus of the DS.

The solution to Eq. (5) is

$$\varphi(z, t) = f(z - \beta t) + g(z + \beta t) \tag{6}$$

expressed through the phase variables $u = z - \beta t$ and $w = z + \beta t$. In Eq. (6), $f(z - \beta t)$ is the torsional wave emanating upward from the bit, $g(z + \beta t)$ is the torsional wave descending to the bit from the top end of the DS (Fig. 1(b)), and $\beta = \sqrt{G/\rho}$ is the torsion wave velocity.

The boundary condition at the top end $z = L$ of the DS is regarded as a clamping end, i.e.

$$\varphi(L, t) = 0 \text{ or } f(L - \beta t) + g(L + \beta t) = 0 \tag{7}$$

Meanwhile, the boundary condition at the lower end of the bit rotating can be represented in the following form

$$M^{in} + M^{fr} + M^{el} = 0 \tag{8}$$

Here, $M^{in} = -J \cdot \ddot{\varphi}$ is the moment of inertia forces acting on the bit; $M^{el} = GI_z \partial\varphi/\partial z$ is the moment of elastic forces acting on the bit; $M^{fr} = M^{fr}(\omega + \dot{\varphi})$ is the cutting moment or the moment of friction forces formed between the bit and broken rock. Inasmuch as independent variables z and t are connected by phase variables u and w, the partial derivative $\partial\varphi/\partial z$ can be expressed through the $\partial\varphi/\partial t$ derivative. Indeed, it follows from Eq. (6)

$$\begin{aligned} \frac{\partial \varphi}{\partial z} &= \frac{\partial f}{\partial u} \cdot \frac{\partial u}{\partial z} + \frac{\partial g}{\partial w} \cdot \frac{\partial w}{\partial z} = \frac{\partial f}{\partial u} + \frac{\partial g}{\partial w} \\ \frac{\partial \varphi}{\partial t} &= \frac{\partial f}{\partial u} \cdot \frac{\partial u}{\partial t} + \frac{\partial g}{\partial w} \cdot \frac{\partial w}{\partial t} = -\frac{\partial f}{\partial u}\beta + \frac{\partial g}{\partial w}\beta \end{aligned} \tag{9}$$

Comparing the right-hand sides of these equalities, one can write

$$\frac{\partial \varphi}{\partial z} = -\frac{1}{\beta}\frac{\partial f}{\partial t} + \frac{1}{\beta}\frac{\partial g}{\partial t}$$

and express the M^{el} moment in terms of the variable t. After some substitutions and rearrangements, Eq. (8) can be changed to the following form (Gulyaev *et al.* 2010)

$$J[\ddot{f}(-\beta t) - \ddot{f}(-\beta t + 2L)] + \frac{GI_z}{\beta}[\dot{f}(-\beta t) + \dot{f}(-\beta t + 2L)] - M^{fr}(\omega + \dot{\varphi}) = 0 \tag{10}$$

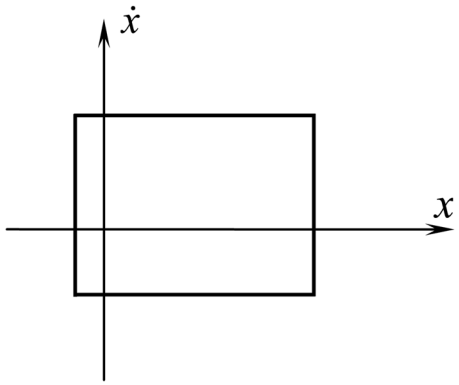

Fig. 3 Typical phase portrait of relaxation vibration

where $f = f(0,t)$, $\varphi = \varphi(0,t)$. The function M^{fr} will be constructed later.

The solutions of the equation possess a series of features derived from the structure of the function $M^{fr}(\omega + \dot{\varphi})$. First and foremost, it has a stationary solution $f(t) = const$ or $\varphi(t) = const$ for any value of ω. Besides, a diapason $\omega_b \le \omega \le \omega_l$ exists, where stable non-stationary periodic solutions occur in addition to constant ones, which become unstable. Outside this diapason, the stationary solutions in the form of balanced rotation $\omega = const$, $\varphi = const$ are stable. The states $\omega = \omega_b$, $\omega = \omega_l$, where the stationary rotation is changed by autovibration and vice versa, are called the bifurcations of limit cycle birth and limit cycle loss or the Hopf bifurcations.

The second peculiarity of Eq. (10) is associated with small values of inertia moment J of the bit in comparison with values GI_z/β and M^{fr}. So, as indicated above, the problem of integrating this equation is singularly perturbed, the autovibrations are of relaxation type and have nearly discontinuous velocities.

Finally, a further trait of Eq. (10) is that it contains the delay argument $-\beta(t - 2L/\beta)$. Owing to this, the system remembers the perturbations imposed previously on it with the $2L/\beta$ delay and is tuned to quantized vibrations with time quantum $\Delta\tau = 2L/\beta$ (Gulyaev *et al.* 2010). So, it is of interest to trace the evolution of the autovibration modes with the change in parameter ω.

3. Evolution of autovibration modes with the drill string rotation velocity change

One of the basic peculiarities, making critical impact on the process of the torsional vibration self-excitation and its peculiarities, is the law of cutting (friction) moment M^{fr} dependence on the total angular velocity $\omega + \dot{\varphi}$ of the bit rotation.

The shape of function $M^{fr}(\omega + \dot{\varphi}) = M^{fr}(\dot{\theta})$ is determined by many factors, including the bit structure and its diameter, the bit chisel material (high-strength steel or diamonds) and wear of the chisels, the force of the bit pressure on the bore-hole bottom, mechanical properties of the rock drilled (strength, plasticity, brittleness, etc), as well as composition of the washing liquid. The presented factors are not only extremely diversified, but their numerical values vary during the drilling process. So, it is evident that there are no universally valid friction moment functions, and what is more, they even cannot be constructed with sufficient accuracy.

Consequently, it is conceivable that the universal functions of this kind are not necessary and it is

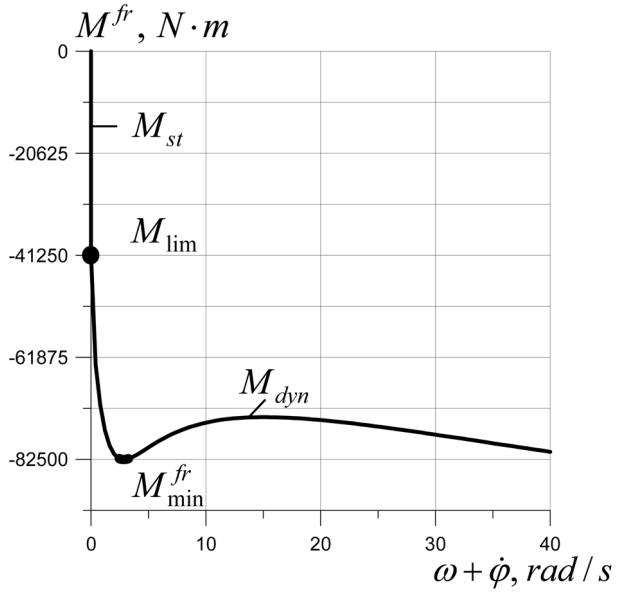

Fig. 4 Total angular velocity dependence of frictional moment M^{fr} ($M^{fr}_{\min} = -82500$ N · m, $k = 0.025$, $c = 1$, $\omega = 2.85$ rad/s)

sufficient to consider only some general and typical phenomena encountered by the drilling processes and to find conditions and limits of their existence. As it will be shown below, usually only the extremum points of these functions are of primary interest for the stability analysis.

The most commonly encountered relationships between M^{fr} and $\omega + \dot{\varphi}$ are represented by the Coulomb friction law (Tucker and Wang, 1999). It is used in our investigation for analysis of general regularities of autovibration proceedings. In its diagram (Fig. 4), the vertical segment determines the static friction moment M_{st}, it is realized in the absence of sliding between bodies. After achieving some limit value $M_{\lim}$, the static friction moment M_{st} is replaced by the dynamic friction moment M_{dyn}, which is accompanied by sliding between rubbing surfaces.

As our calculations will testify, during the auto-oscillation only the lower parts of these functions are involved in the friction process. So, the bit vibrations do not depend on the static segment existing in the M^{fr} function and the dynamic friction moment M_{dyn} can be represented with the aid of the following approximate function

$$M^{fr} = M_{\lim} - c\sqrt{M_{vis}} \tag{11}$$

Here, the viscous component is approximated by the expression

$$M_{vis} = m\left(\frac{a_1 k(\omega+\dot{\varphi}) + a_3 k^3(\omega+\dot{\varphi})^3 + a_5 k^5(\omega+\dot{\varphi})^5 + a_7 k^7(\omega+\dot{\varphi})^7 + a_9 k^9(\omega+\dot{\varphi})^9}{1 + a_2 k^2(\omega+\dot{\varphi})^2}\right) \tag{12}$$

where the coefficients a_i $(i = 1, 2, \ldots, 9)$ are found by the trial-and-error method. This type of friction is inherent in the cases when sliding between the bodies begins under certain limit value of the applied moment.

Table 1 Values of parameters of the homogeneous drill string auto-oscillations

($M^{fr}_{\min} = -82500\ \mathrm{N \cdot m}, k = 0.025, c = 1$)

ω	$\omega_b < \omega < \omega_l$										
(rad / s)	2.85	2.86	2.87	6	10	15	17	18	19	19.6	19.9
φ_{st} (rad)	-32.68	-32.69	-32.71	-32.32	-32.25	-34.51	-35.82	-29.65	-29.65	-29.67	-29.68
φ_{av} (rad)	-32.61	-32.58	-29.43	-29.25	-29.49	-30.38	-31.03	-29.44	-29.49	-29.53	-29.55
D (rad)	0.16	0.24	6.61	6.12	5.53	8.25	9.55	0.43	0.33	0.29	0.27
T (s)	1.28	1.27	2.91	1.86	1.25	1.26	1.28	1.31	1.25	1.25	1.19

In calculation, the following values are used for the characteristic parameters: $G = 8.077 \cdot 10^{10}$ Pa, $\rho = 7.8 \cdot 10^3\ \mathrm{kg/m^3}$, $J = 3.1\ \mathrm{kg/m^2}$, $L = 1000$ m. External and internal diameters of the tube cross-section are $d_1 = 0{,}1483$ m, $d_2 = 0{,}1683$ m, so $I_z = 3.12 \cdot 10^{-5}\ \mathrm{m^4}$. In Eq. (11), the coefficients of the function of the M^{fr} moment shown in Fig. 4 have the following values $a_1 = 2400\ \mathrm{N \cdot m \cdot s}$, $a_2 = 225\ \mathrm{s^2}$, $a_3 = 15000\ \mathrm{N \cdot m \cdot s^3}$, $a_5 = 1\ \mathrm{N \cdot m \cdot s^5}$, $a_7 = 4\ \mathrm{N \cdot m \cdot s^7}$, $a_9 = -130\ \mathrm{N \cdot m \cdot s^9}$, $M_{\lim} = -14250\ \mathrm{N \cdot m}$, $M^{fr}_{\min} = -82500\ \mathrm{N \cdot m}$, $k = 0.025$, $m = 1000$, $c = 1$.

In the process of functioning, the DS can be either in the states of stationary rotation or of torsional self-excited elastic oscillation, depending on the chosen regime of drilling. Types of these states are dictated by the Eq. (10) solutions, which are primarily determined by the function in Eq. (11) and angular velocity ω, as compared with the value ω_m of the M^{fr} minimum, whose position is determined by the values of parameter k.

The investigation was performed by integrating Eq. (10) by the Runge-Kutta method with the initial conditions $\varphi(0) = 0$, $\dot{\varphi}(0) = 0$ for different values of ω. The integration step is selected to be $\Delta t = 7.769 \cdot 10^6$ s.

The results of the numerical investigation are presented in Table 1. Their analysis permits us to formulate some regularities. The most important conclusion is that the value ω_b of the angular velocity ω corresponding to the bifurcation state of the limit cycle birth equals the value $\omega_b = 2.85\ \mathrm{rad/a}$, which conforms to the minimum point of the $M^{fr}(\omega + \dot{\varphi})$ diagram. The regimes of motion with $|\omega| < \omega_b$ are characterized by the stationary rotation without any oscillation when the system changes from its initial state $\varphi(0) = 0$, $\dot{\varphi}(0) = 0$ to some quasi-static equilibrious state $\varphi(t) = \varphi_{st}$, $\dot{\varphi}(t) = 0$ and self-excited vibrations do not take place. But during the system transition from outside to inside this diapason through the value $\omega = \omega_b$, the Hopf bifurcation occurs and limit cycles appear together with the unstable stationary solutions $\varphi(t) = const$, $\dot{\varphi}(t) = 0$. The autovibrations occur relative to some mean (averaged) value φ_{av} with swing D and period T. Stability of the born limit cycles was confirmed by immediate computer simulation.

Figs. 5-7 illustrate the torsional oscillations of the DS bit at the state of the limit cycle birth ($\omega = 2.85$ rad / s). Firstly, they vibrate with small swing $D = 0.155$ rad and period $T = 1.275$ s. Their progression from the initial state $\varphi(0) = 0$, $\dot{\varphi}(0) = 0$ is shown in Fig. 5. Large scale of these vibrations (Fig. 6) allows us to conclude that they have the relaxation mode with nearly discontinuous angular velocity $\dot{\varphi}$ (Fig. 7). It is interesting to note that they are realized in a small

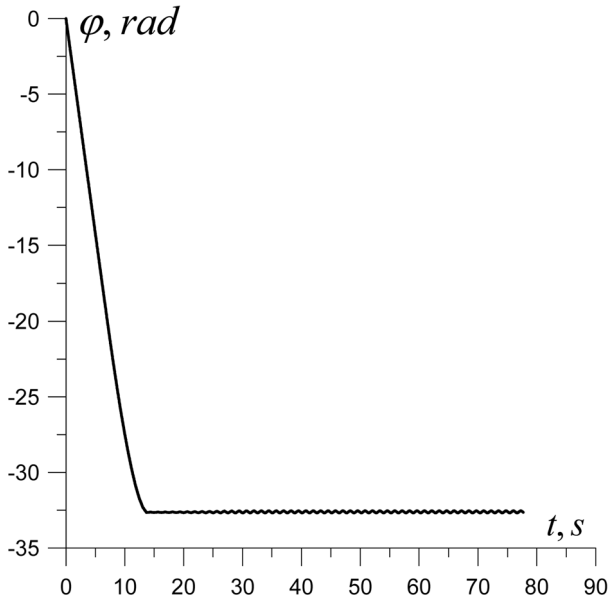

Fig. 5 Torsional auto-oscillation excitation of the bit at the state of limit cycle birth ($M^{fr}_{\min} = -82500\ \mathrm{N \cdot m}$, $k = 0.025$, $c = 1$, $\omega = 2.85\ \mathrm{rad/s}$)

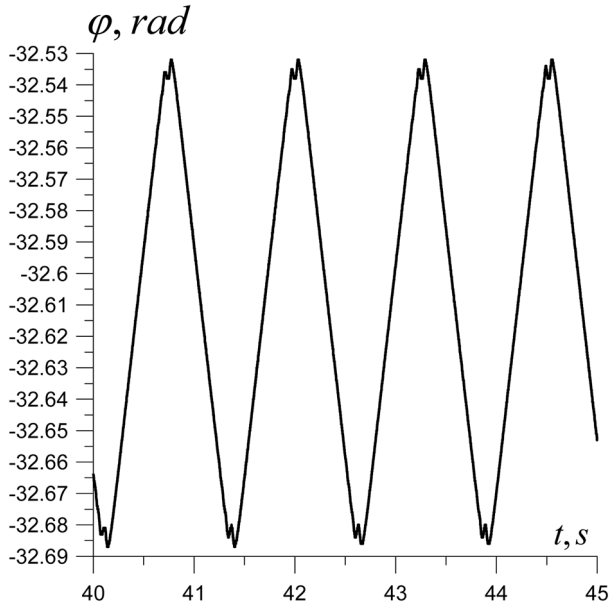

Fig. 6 Torsional auto-oscillation on a large scale ($M^{fr}_{\min} = -82500\ \mathrm{N \cdot m}$, $k = 0.025$, $c = 1$, $\omega = 2.85\ \mathrm{rad/s}$)

vicinity of the extremum point ω_b in the $M^{fr}(\omega + \dot{\varphi})$ diagram. In Fig. 4 it is separated by small segment of solid line.

The mode of self-excited vibrations of the bit evolves as the ω value increases. In so doing, the

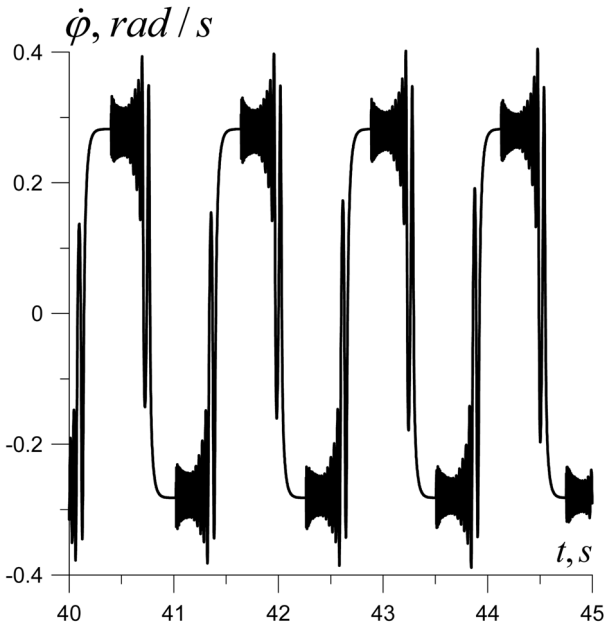

Fig. 7 Angular velocity $\dot{\varphi}$ of the bit versus time t ($M_{\min}^{fr} = -82500\ \mathrm{N \cdot m}$, $k = 0.025$, $c = 1$, $\omega = 2.85$ rad / s)

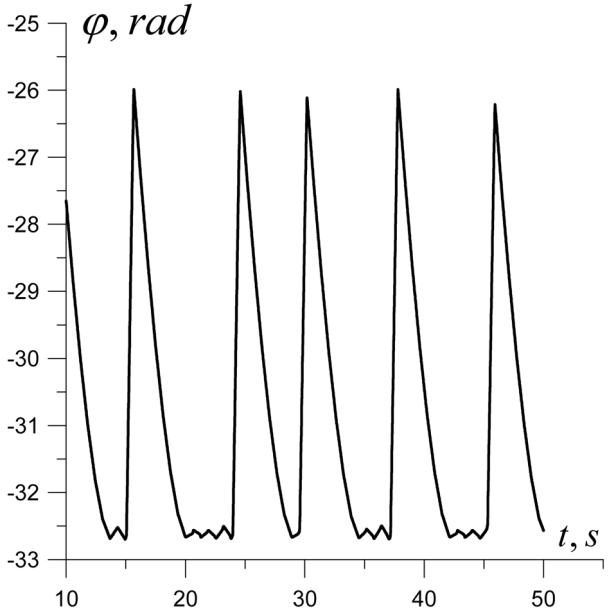

Fig. 8 Elastic torsional angle φ versus time t ($M_{\min}^{fr} = -82500\ \mathrm{N \cdot m}$, $k = 0.025$, $c = 1$, $\omega = 2.87$ rad / s)

parameter D also increases but the period T practically remains unchanged (see Table 1). The function $\varphi(t)$ for $\omega = 2.87$ rad / s can be seen in Fig. 8, with the quantized segments of the $\dot{\varphi}(t)$

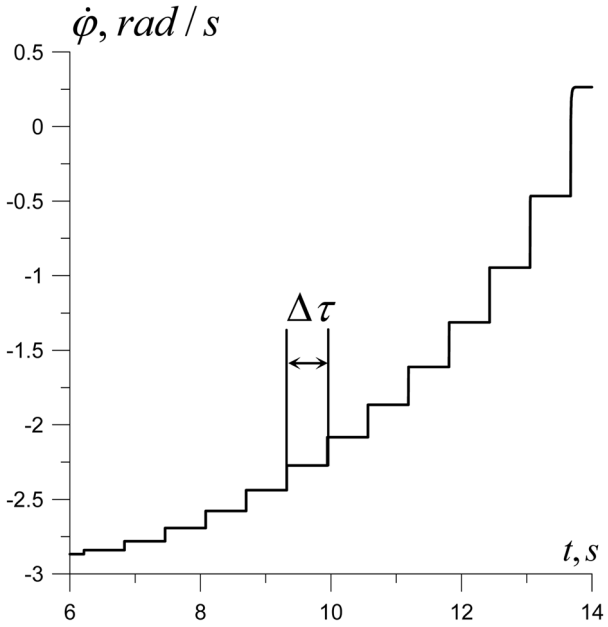

Fig. 9 Large-scale view of quantized change of the bit's torsional velocity ($M^{fr}_{\min} = -82500\ \mathrm{N \cdot m}$, $k = 0.025$, $c = 1$, $\omega = 2.87\ \mathrm{rad/s}$)

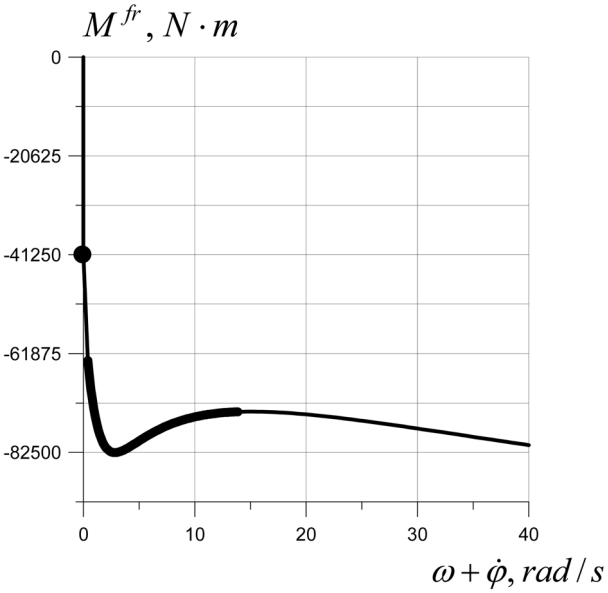

Fig. 10 Domain of auto-oscillation on $M^{fr}(\omega + \dot{\varphi})$ diagram ($M^{fr}_{\min} = -82500\ \mathrm{N \cdot m}$, $k = 0.025$, $c = 1$, $\omega = 2.87\ \mathrm{rad/s}$)

function shown in Fig. 9. In this case, the motion is not periodic and the segment of total angular velocity $\omega + \dot{\varphi}$ covers the longer part of the $M^{fr}(\omega + \dot{\varphi})$ diagram (Fig. 10).

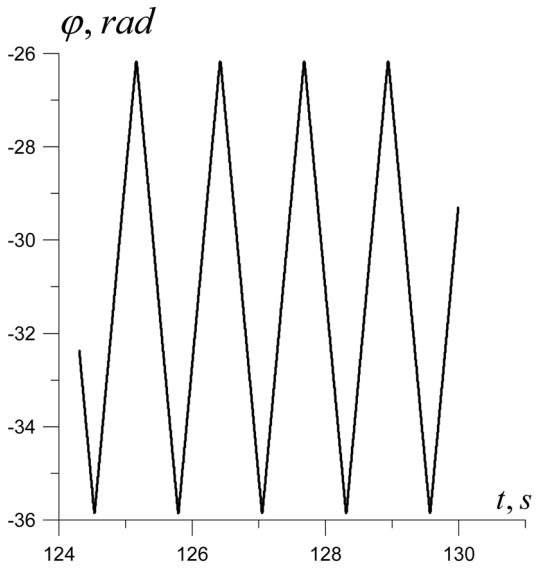

Fig. 11 Elastic torsional angle φ versus time t ($M_{\min}^{fr} = -82500\ \mathrm{N}\cdot\mathrm{m}$, $k = 0.025$, $c = 1$, $\omega = 17\ \mathrm{rad/s}$)

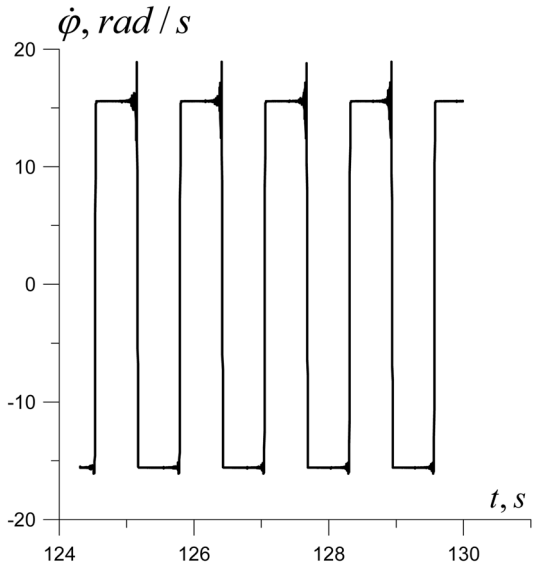

Fig. 12 Angular velocity $\dot{\varphi}$ of the bit versus time t ($M_{\min}^{fr} = -82500\ \mathrm{N}\cdot\mathrm{m}$, $k = 0.025$, $c = 1$, $\omega = 17\ \mathrm{rad/s}$)

The relaxation mode of vibrations acquires more distinct character for $\omega = 17\ \mathrm{rad/s}$. The function $\varphi(t)$ gains the shape of triangular sine (Fig. 11), while the function $\dot{\varphi}(t)$ becomes nearly as the rectangular cosine (Fig. 12). The phase portrait also assumes appropriate outline (compare Figs. 13 and 3).

At the state of bifurcation of the limit cycle loss ($\omega_l = 19.9\ \mathrm{rad/s}$ in the Table 1), the auto-

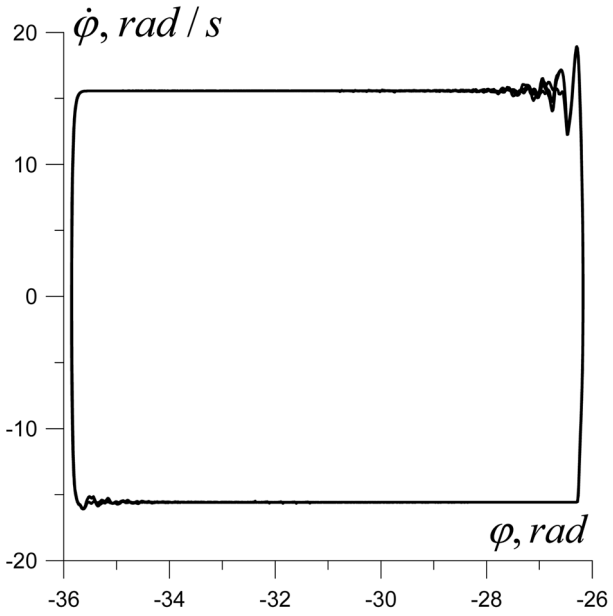

Fig. 13 Phase portrait of torsional auto-oscillation ($M^{fr}_{\min} = -82500\ \mathrm{N \cdot m}$, $k = 0.025$, $c = 1$, $\omega = 17\ \mathrm{rad/s}$)

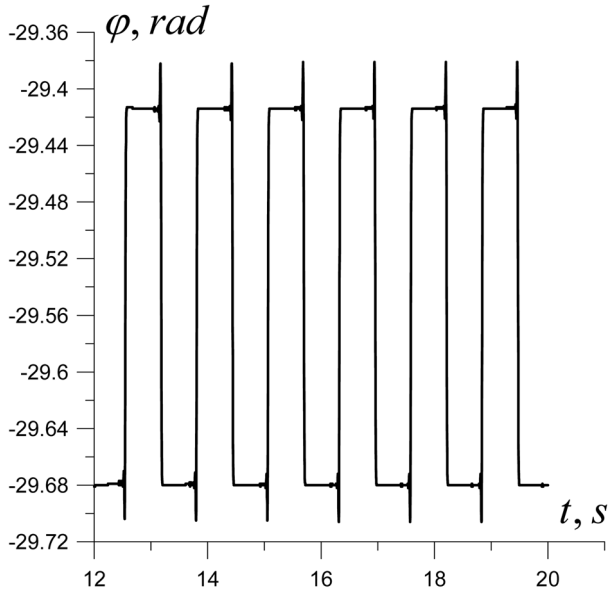

Fig. 14 Elastic torsion auto-oscillation at the state of limit cycle loss ($M^{fr}_{\min} = -82500\ \mathrm{N \cdot m}$, $k = 0.025$, $c = 1$, $\omega = 19.9\ \mathrm{rad/s}$)

oscillations again proceed with small swings (Fig. 14), but the function $\varphi(t)$ became nearly discontinuous with large values of angular velocity $\dot{\varphi}(t)$. So, in the diagram for $M^{fr}(\omega + \dot{\varphi})$, the

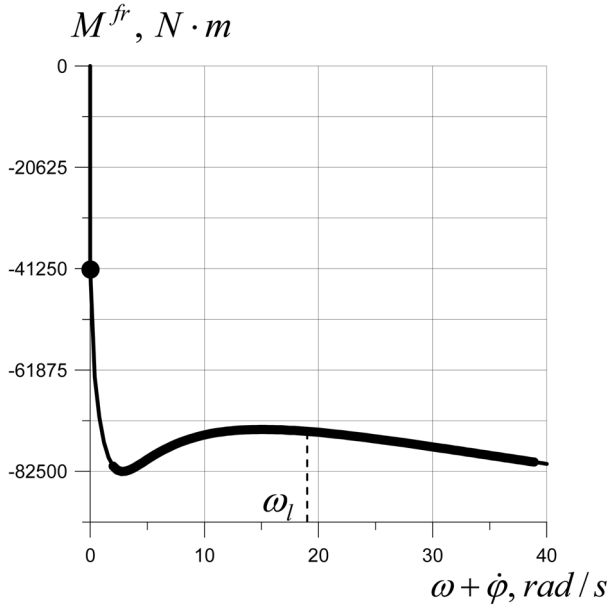

Fig. 15 Domain of auto-oscillation on $M^{fr}(\omega + \dot{\varphi})$ diagram ($M^{fr}_{\min} = -82500\ \mathrm{N \cdot m}$, $k = 0.025$, $c = 1$, $\omega = 19.9\ \mathrm{rad/s}$)

Table 2 Values of parameters of the homogeneous drill string auto-oscillations ($k = 0.1$, $M^{fr}_{\min} = -82500\ \mathrm{N \cdot m}$ and $M^{fr}_{\min} = -165000\ \mathrm{N \cdot m}$)

	$M^{fr}_{\min} = -82500\ \mathrm{N \cdot m}$, $k = 0.1, c = 1$		$M^{fr}_{\min} = -165000\ \mathrm{N \cdot m}$, $k = 0.1, c = 2$	
$\omega\ (\rho\alpha\delta/\sigma)$	ω_b	ω_l	ω_b	ω_l
	0.71	3.775	0.71	3.775
φ_{st} (rad)	-32.63	-33.27	-78.75	-79.58
φ_{av} (rad)	-30.56	-31.19	-74.28	-74.42
D (rad)	4.13	4.17	8.95	10.33
T (s)	13.64	2.49	34.33	6.59

segment of auto-oscillations covers a larger part of the curve (compare Fig. 15 for the limit cycle loss bifurcation with Fig. 4 for the limit cycle birth bifurcation).

Besides, as shown by Gulyaev *et al.* (2010), in the considered examples, the auto-oscillations are quantized in time with the time quantum $\Delta\tau = 2L/\beta \approx 0.6215$ s. Inside this segment of time, the angular velocity $\dot{\varphi}(t)$ is nearly constant.

It is of interest to trace the change of the autovibration process parameters for various values k, $M^{fr}_{\min}$, c, and comparing the function M^{fr} calculated by Eqs. (11) and (12). In Table 2, the calculation results are represented for the cases $k = 0.1$, $c = 1$, $M^{fr}_{\min} = -82500\ \mathrm{N \cdot m}$ and $k = 0.1$, $c = 2$, $M^{fr}_{\min} = -165000\ \mathrm{N \cdot m}$. They testify that a fourfold increase of k to the value $k = 0.1$ leads to nearly a fourfold decrease of the ω_b value and eightfold reduction of ω_l (compare Tables 1 and 2).

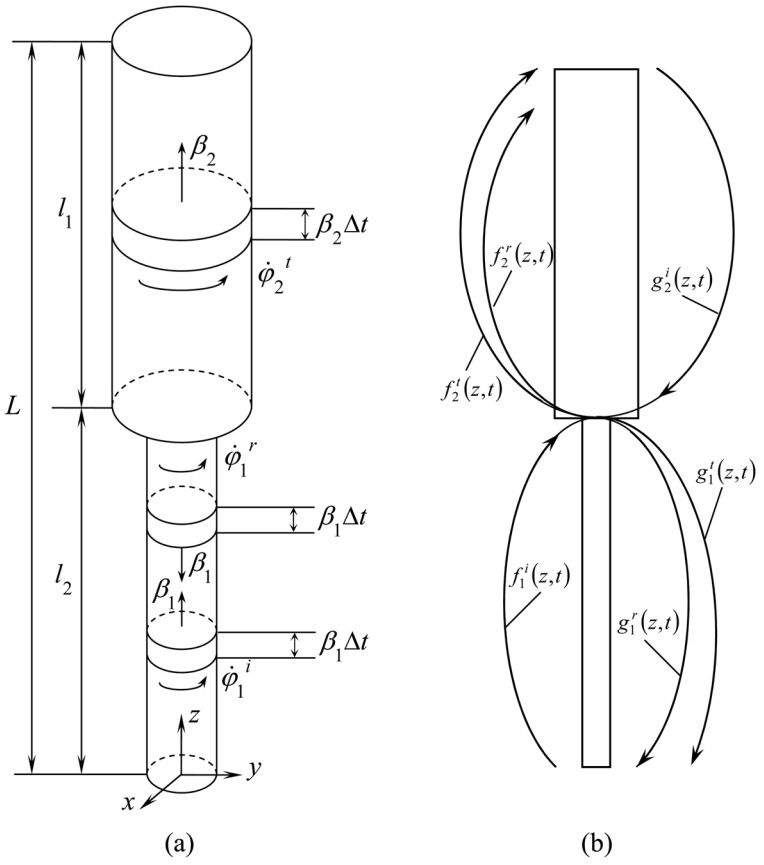

Fig. 16 Schematic of torsional wave propagation in a sectional drill string: (a) fragmentation of an incident wave and (b) wave diffraction at the interface point

The limit cycles of the torsion wave pendulum vibrations do not depend on the initial conditions, so the self-excitation has the soft character.

4. Statement of the problem about torsional auto-vibrations of sectional drill strings

If mechanical characteristics of a DS change along its axial line, the waves $f(z-\beta t)$ and $g(z+\beta t)$ transform in their propagation and Eq. (10) loses its meaning. To solve the problem, it is necessary to build the function $g(0+\beta t)$ at the lower end $z = 0$ for every specific case and to use the appropriate functions $\dot{g}(\beta t)$, $\ddot{g}(\beta t)$ in Eq. (10), instead of the variables $\ddot{f}(-\beta t+2L)$, $\dot{f}(-\beta t+2L)$.

Let, for example, the DS consists of two sections as shown in Fig. 16 with lengths l_1, l_2 and mechanical characteristics β_1, ρ_1, I_1 and β_2, ρ_2, I_2, respectively. Then, the components of the $f(z-\beta t)$ waves, propagating from the point $z = 0$ and reaching the point $z = l_1$, will experience the action of impact reflection-refraction (transmission). To calculate the intensities of the reflected

and transmitted waves, consider the process of diffr action of the wave component of length $\beta_1 \Delta t$ during the time interval Δt. Separate the DS elements into the incident, reflected and transmitted waves, which take part in this interaction and have the angular velocities $\dot{\varphi}_1^i, \dot{\varphi}_1^r, \dot{\varphi}_2^t$ and lengths $\beta_1 \Delta t, \beta_1 \Delta t, \beta_2 \Delta t$, respectively (Fig. 16(a)). Here, the top indices i, r, t denote the incident, reflected and transmitted waves, and the lower ciphers 1, 2 indicate the DS section number. Considering the $\dot{\varphi}_1^i$ velocities to be known, we can calculate the $\dot{\varphi}_1^r, \dot{\varphi}_2^t$ velocities. For this purpose, use the condition of conservation of the momentum of each separate element before and after impact. One can write

$$\Delta K_1^i = \Delta K_1^r + \Delta K_2^t \tag{13}$$

where

$$\begin{aligned} \Delta K_1^i &= \dot{\varphi}_1^i \cdot \rho_1 I_1 \beta_1 \Delta t \\ \Delta K_1^r &= \dot{\varphi}_1^r \cdot \rho_1 I_1 \beta_1 \Delta t \\ \Delta K_2^t &= \dot{\varphi}_2^t \cdot \rho_2 I_2 \beta_2 \Delta t \end{aligned} \tag{14}$$

Supplementing Eq. (13) by the condition of angular velocity continuity

$$\dot{\varphi}_1^i + \dot{\varphi}_1^r = \dot{\varphi}_2^t \tag{15}$$

one obtains the system of two equations for calculation of $\dot{\varphi}_1^r$ and $\dot{\varphi}_2^t$. The solution is

$$\begin{aligned} \dot{\varphi}_1^r &= \frac{\beta_2 \rho_2 I_2 - \beta_1 \rho_1 I_1}{\beta_1 \rho_1 I_1 + \beta_2 \rho_2 I_2} \dot{\varphi}_1^i \\ \dot{\varphi}_2^t &= \frac{2 \beta_1 \rho_1 I_1}{\beta_1 \rho_1 I_1 + \beta_2 \rho_2 I_2} \dot{\varphi}_1^i \end{aligned} \tag{16}$$

The torsional angles in the reflected and transmitted waves can be found from the conditions of continuity for torques and torsional angles at $z = l_1$. They are as follows

$$\begin{aligned} \varphi_1^r &= \frac{\beta_2 \rho_2 I_2 - \beta_1 \rho_1 I_1}{\beta_1 \rho_1 I_1 + \beta_2 \rho_2 I_2} \varphi_1^i \\ \varphi_2^t &= \frac{2 \beta_1 \rho_1 I_1}{\beta_1 \rho_1 I_1 + \beta_2 \rho_2 I_2} \varphi_1^i \end{aligned} \tag{17}$$

Considering the diffraction of the $g(z + \beta t)$ wave at the point $z = l_1$, the $g_2^i(z + \beta_2 t)$ wave in the second section, arriving at this point, is considered to be incident and known, but the reflected $g_2^r(z - \beta_2 t)(z \geq l_1)$ and transmitted $g_1^t(z + \beta_1 t)(z \leq l_1)$ waves should be determined. Their kinematical characteristics are calculated by the foregoing techniques through the use of the formulae below

$$\dot{\varphi}_2^r = \frac{\beta_1\rho_1 I_1 - \beta_2\rho_2 I_2}{\beta_1\rho_1 I_1 + \beta_2\rho_2 I_2}\dot{\varphi}_2^i$$

$$\dot{\varphi}_1^t = \frac{2\beta_2\rho_2 I_2}{\beta_1\rho_1 I_1 + \beta_2\rho_2 I_2}\dot{\varphi}_2^i \tag{18}$$

$$\varphi_2^r = \frac{\beta_1\rho_1 I_1 - \beta_2\rho_2 I_2}{\beta_1\rho_1 I_1 + \beta_2\rho_2 I_2}\varphi_2^i$$

$$\varphi_1^t = \frac{2\beta_2\rho_2 I_2}{\beta_1\rho_1 I_1 + \beta_2\rho_2 I_2}\varphi_2^i \tag{19}$$

The correlations (16), (17) and (18), (19) satisfy the obvious conditions occurring in marginal cases. For example, Eqs. (16), (17) testify that, if two sections have the same geometrical and mechanical properties, then $\dot{\varphi}_1^r = 0$, $\dot{\varphi}_2^t = \dot{\varphi}_1^i$ and $\varphi_1^r = 0$, $\varphi_2^t = \varphi_1^i$. When the second section is absolutely rigid, its $\beta_2\rho_2 I_2 \to \infty$ and $\dot{\varphi}_1^r = \dot{\varphi}_1^i$, $\dot{\varphi}_2^t = 0$, $\varphi_1^r = \varphi_1^i$, $\varphi_2^t = 0$. If the acoustic rigidity of the second section reduces to zero, one has $\dot{\varphi}_1^r = -\dot{\varphi}_1^i$, $\dot{\varphi}_2^t = 2\dot{\varphi}_1^i$ and $\varphi_1^r = -\varphi_1^i$, $\varphi_2^t = 2\varphi_1^i$.

As the result of diffractions of the waves $\varphi_1^i(z-\beta_1 t)$ and $\varphi_2^i(z+\beta_2 t)$, the superposition of the transmitted $\varphi_2^t(z-\beta_2 t)$ and reflected $\varphi_2^r(z-\beta_2 t)$ waves will make up the $f_2(z-\beta_2 t)$ function in the second section and the sum $\varphi_1^r(z+\beta_1 t)+\varphi_1^t(z+\beta_1 t)$ will produce the $g_1(z+\beta_1 t)$ function in the first one (Fig. 16(b)). With the allowance made for these rearranging, the initial conditions

$$f_2(l_1-\beta_2 t) = \frac{2\beta_1\rho_1 I_1}{\beta_1\rho_1 I_1 + \beta_2\rho_2 I_2}f_1^i(l_1-\beta_1 t) - \\ -\frac{\beta_1\rho_1 I_1 - \beta_2\rho_2 I_2}{\beta_1\rho_1 I_1 + \beta_2\rho_2 I_2}g_2^i(l_1+\beta_1 t)$$

$$\dot{f}_2(l_1-\beta_2 t) = \frac{2\beta_1\rho_1 I_1}{\beta_1\rho_1 I_1 + \beta_2\rho_2 I_2}\dot{f}_1^i(l_1-\beta_1 t) - \\ -\frac{\beta_1\rho_1 I_1 - \beta_2\rho_2 I_2}{\beta_1\rho_1 I_1 + \beta_2\rho_2 I_2}\dot{g}_2^i(l_1+\beta_1 t) \tag{20}$$

can be formulated for the $f_2(z-\beta_2 t)$ wave at the boundary $z = l_1$ of the domain $l_1 \le z \le L$, and the initial conditions

$$g_1(l_1+\beta_1 t) = \frac{\beta_1\rho_1 I_1 - \beta_2\rho_2 I_2}{\beta_1\rho_1 I_1 + \beta_2\rho_2 I_2}f_1^i(l_1-\beta_1 t) + \\ + \frac{2\beta_2\rho_2 I_2}{\beta_1\rho_1 I_1 + \beta_2\rho_2 I_2}g_2^i(l_1+\beta_2 t)$$

$$\dot{g}_1(l_1+\beta_1 t) = \frac{\beta_1\rho_1 I_1 - \beta_2\rho_2 I_2}{\beta_1\rho_1 I_1 + \beta_2\rho_2 I_2}\dot{f}_1^i(l_1-\beta_1 t) + \\ + \frac{2\beta_2\rho_2 I_2}{\beta_1\rho_1 I_1 + \beta_2\rho_2 I_2}\dot{g}_2^i(l_1+\beta_2 t) \tag{21}$$

for the $g_1(z+\beta_1 t)$ wave at the same point of the domain $0 \le z \le l_1$.

Eqs. (5), (6), together with boundary conditions (7), (8) and continuity conditions (20), (21), describe the three-point boundary problem relative to the independent variable z with the boundary conditions at the points $z = 0$, $z = l_1$ and $z = L$. These equations, combined with appropriate initial conditions, represent the Cauchy problem. It can be solved by the Runge - Kutta method.

5. Torsional autovibrations of sectional drill strings

To embrace more emphatically the stated questions and to test the proposed approach, the relationship between the modes of the drill string autovibration and the existence of sections with different mechanical properties in the drill string was analyzed. Four cases were considered for the drill string of $L = 1000$ m with two sections of the following lengths: 1) $l_1 = L$, $l_2 = 0$; 2) $l_1 = 2L/3$, $l_2 = L/3$; 3) $l_1 = L/2$, $l_2 = L/2$; 4) $l_1 = L/3$, $l_2 = 2L/3$. The tube of the first section has the geometrical and mechanical parameters assumed in Section 3. The second section tube has diameters $d_1 = 0{,}08898$ m, $d_2 = 0{,}10098$ m, so its $I_z = 3.12 \cdot 10^{-5}$ m^4.

First of all, it is necessary to stress that in all the cases considered, the states of the autovibration birth do not depend on the drill string structure and occur at $\omega_b \approx 0.71$ rad/s.

The results of calculation for the angular velocity value $\omega = 2$ rad/s picked from the segment $\omega_b < \omega < \omega_l$ are given in Table 3. They are grouped into four columns corresponding to the four cases considered. Recall the designations used. Here, φ_{st} is the torsional angle of the drill string at its limit state of quasi-static equilibrium; φ_{av} is the averaged elastic torsional angle; D is the swing of the autovibration angle; and T is the autovibration period. The variation of the torsional angle with respect to time for the drill column with sections $l_1 = L/3$, $l_2 = 2L/3$ is shown in Fig. 17.

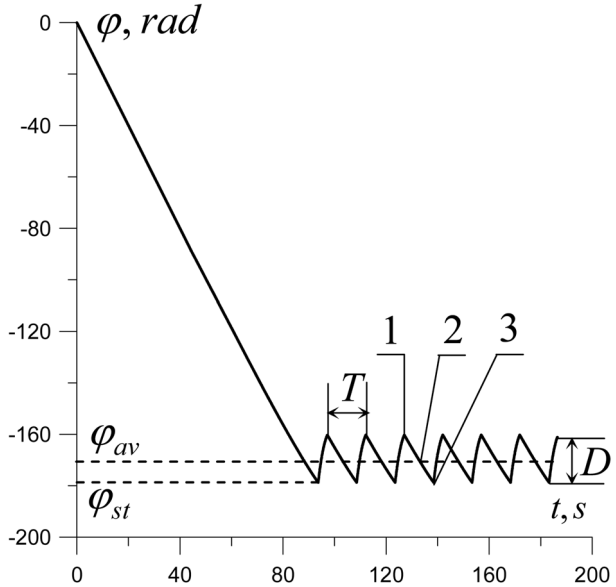

Fig. 17 Torsional auto-oscillation excitation of the bit at the state of limit cycle birth ($M^{fr}_{\min} = -82500$ N·m, $k = 0.1$, $c = 1$, $\omega = 2$ rad/s)

Table 3 Values of parameters of the sectional drill string auto-oscillations

($M_{\min}^{fr} = -82500\ \mathrm{N \cdot m}$, $k = 0.1, c = 1$)

	1	2	3	4
	$l_1 = L, l_2 = 0$	$l_1 = 2L/3, l_2 = L/3$	$l_1 = L/2, l_2 = L/2$	$l_1 = L/3, l_2 = 2L/3$
φ_{st} (rad)	-33.02	-105.23	-142.05	-178.75
φ_{av} (rad)	-30.97	-100.24	-134.79	-169.42
D (rad)	4.11	9.95	14.53	18.65
T (s)	2.78	8.33	11.63	14.95

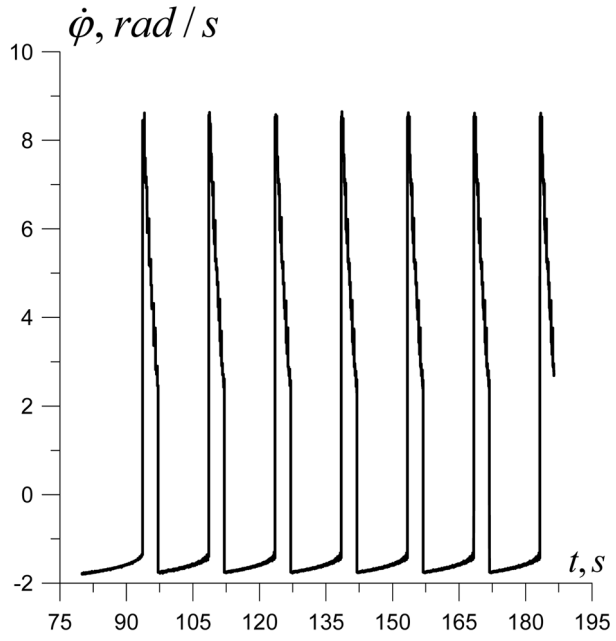

Fig. 18 Angular velocity $\dot{\varphi}$ of the bit versus time t ($M_{\min}^{fr} = -82500\ \mathrm{N \cdot m}$, $k = 0.1$, $c = 1$, $\omega = 2\ \mathrm{rad/s}$)

Referring to Table 3, one can see that all the dynamic characteristics have the tendency to increase with the enlargement in l_2. This is attributed to the fact that the total torsional stiffness of the drill string decreases as the segment l_2 grows.

At the same time, substitution of the sectional drill columns for the homogeneous ones entails also essential change of their vibration modes due to the additional destruction effect of the torsional wave profile at the point of discontinuity of the torsion waveguide stiffness. To gain more insight into this phenomenon, the variation of the bit angular velocity $\dot{\varphi}$ with respect to time t is shown in Fig. 18, which differs from the functions $\dot{\varphi}(t)$ displayed in Figs. 7 and 12 and is distinguished by the sharp change of slow and fast motions. Part of this diagram is enlarged in Fig. 19. In this case, the motion is also quantized with respect to time with quantum duration $\Delta\tau = 0.6125\ \mathrm{s}$, but the velocity - time portions are fragmented and less regularized, because inside every global quantum, there are three additional subquanta. They are conditioned by additional diffraction of the wave at the internal interface point.

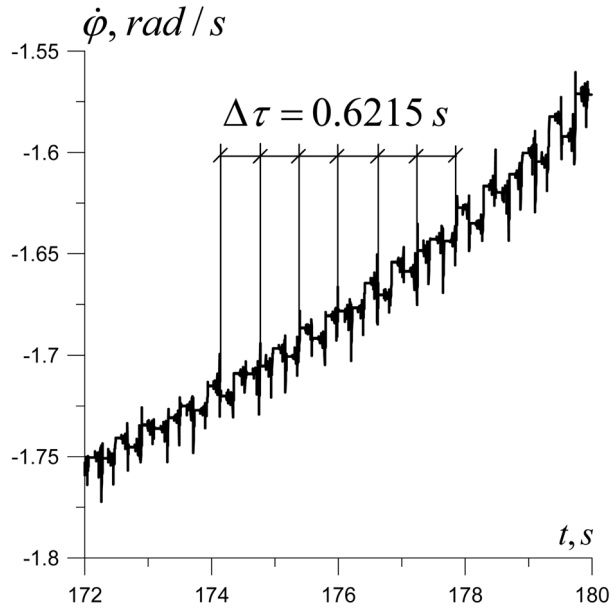

Fig. 19 Large-scale view of fragmented quantized change of the bit's torsional velocity ($M_{\min}^{fr} = -82500\ \mathrm{N \cdot m}$, $k = 0.1$, $c = 1$, $\omega = 2\ \mathrm{rad/s}$)

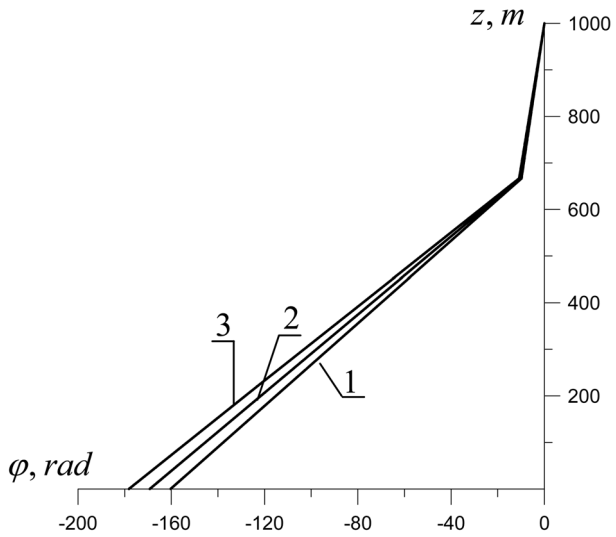

Fig. 20 Modes of the DS twist

The interface point is also the basic cause of the torsional wave transmission along the DS axis, which is illustrated in Fig. 20. Brocken curves 1, 2, 3 correspond to states 1, 2, 3 in Fig. 17. Additional breaks of the DS twist angle resulting from the quantized character of the vibrations are very small and are not discernible in the scale used.

6. Conclusions

The analysis of the limit cycle birth bifurcations in the torsional wave models of homogeneous and sectional drill strings is presented in this paper. The constitutive differential equations with delay argument are constructed, which is shown to be singularly perturbed. Based on analysis of their solutions, one can draw the following conclusions for the torsional oscillation self-excitation of the drill string:

1. The auto-oscillations of homogeneous and sectional DSs prevail at low values of their angular velocity ω, the boundaries of the ω segments of their self-excitation do not depend on the number of the DS sections and are determined by the outline of the friction moment function.
2. The autovibrations are of the relaxation type and contain fast and slow motions (multiscale motion).
3. The self-excited oscillations proceed in the manner of quantized time. The time quantum durations equal the time of the torsional wave propagating through the doubled length of the DS.
4. The velocity - time quanta in sectional drill strings have additional fragmentations caused by the multiple diffractions of the torsional waves at the points of the section joints.

References

Brett, J.F. (1992), "The genesis of torsional drillstring vibrations", *SPE Drill. Eng.,* **7**, 168-174.

Challamel, N. (2000), "Rock destruction effect on the stability of a drilling structure", *J. Sound Vib*., **233**(2), 235-254.

Chang, K.W. and Howes, F.A. (1984), *Nonlinear singular perturbation phenomena*, Springer-Verlag, New York, Berlin, Heidelberg, Tokyo, 245.

Gulyaev, V.I., Glushakova, O.V. and Hudoliy, S.N. (2010), "Quantized attractors in wave models of torsion vibrations of deep-hole drill strings", *Mech. Solids*, **45**(2), 264-274.

Gulyayev, V.I., Gaidaichuk, V.V., Solovjov, I.L. and Gorbunovich, I.V. (2009), "The buckling of elongated rotating drill strings", *J. Petrol. Sci. Eng*., **67**, 140-148.

Gulyayev, V.I., Khudoliy, S.N. and Andrusenko, E.N. (2011), "Sensitivity of resistance forces to localized geometrical imperfections in movement of drill strings in inclined bore-holes", *Interact. Multiscale Mech*., **4**(1), 3-18.

Hassard, B.D., Kazarinoff, N.D. and Wan, Y.H. (1981), *Theory and applications of Hopf bifurcation*, Cambridge University Press, Cambridge, London, New York, New Rochelle, Melbourne, Sydney, 367.

Kaczmarek, J. (2010), "Collection of dynamical systems with dimensional reduction as a multiscale method of modelling for mechanics of materials", *Interact. Multiscale Mech*., **3**(1), 3-24.

Leine, R.I., Campen, D.H. and Keultjes, W.J.G. (2002), "Stick-slip whirl interaction in drillstring dynamics", *J. Vib. Acoust*., **124**, 209-220.

Mihajlovic, N., van de Wouw, N., Hendriks, M.P.M. and Nijmeijer, H. (2006), "Friction-induced limit cycling in flexible rotor systems: an experimental drill-string set-up", *Nonlinear Dynam.*, **46**(3), 273-291.

Mishchenko, E.F. and Rozov, N.H. (1975), "Differential equations with small parameter and relaxation vibrations", *Nauka*, Moscow, 247. (in Russian)

Shishkin, G.I. and Shishkina, L.P. (2009), *Difference methods for singular perturbation problems*, Russian Academy of Science, Ekaterinburg, CRC Press Taylor & Francis Group Boca Raton, USA, 408.

Tucker, R.W. and Wang, C. (1999), "On the effective control of torsional vibrations in drilling systems", *J. Sound Vib.*, **224**(1), 101-122.

Wang, D. and Fang, L. (2010), "A multiscale method for analysis of heterogeneous thin slabs with irreducible three dimensional microstructures", *Interact. Multiscale Mech*., **3**(3), 213-234.

Zamanian, M., Khadem, S.E. and Ghazavi, M.R. (2007), "Stick-slip oscilations of drag bits by considering damping of drilling mud and active damping system", *J. Petrol. Sci. Eng*., **59**, 289-299.